No difference in kinetics of tau or histone phosphorylation by CDK5/p25 versus CDK5/p35 in vitro

Dylan W. Peterson[a], D. Michael Ando[a], Daryl A. Taketa[a], Hongjun Zhou[b], Fredrick W. Dahlquist[b], and John Lew[a,1]

[a]Departments of Molecular, Cellular, and Developmental Biology and [b]Chemistry, University of California, Santa Barbara, CA 93106

Edited* by John A. Carbon, University of California, Santa Barbara, Santa Barbara, CA, and approved December 16, 2009 (received for review November 5, 2009)

CDK5/p35 is a cyclin-dependent kinase essential for normal neuron function. Proteolysis of the p35 subunit in vivo results in CDK5/p25 that causes neurotoxicity associated with a number of neurodegenerative diseases. Whereas the mechanism by which conversion of p35 to p25 leads to toxicity is unknown, there is common belief that CDK5/p25 is catalytically hyperactive compared to CDK5/p35. Here, we have compared the steady-state kinetic parameters of CDK5/p35 and CDK5/p25 towards both histone H1, the best known substrate for both enzymes, and the microtubule-associated protein, tau, a physiological substrate whose in vivo phosphorylation is relevant to Alzheimer's disease. We show that the kinetics of both enzymes are the same towards either substrate in vitro. Furthermore, both enzymes display virtually identical kinetics towards individual phosphorylation sites in tau monitored by NMR. We conclude that conversion of p35 to p25 does not alter the catalytic efficiency of the CDK5 catalytic subunit by using histone H1 or tau as substrates, and that neurotoxicity associated with CDK5/p25 is unlikely attributable to CDK5 hyperactivation, as measured in vitro.

Alzheimer's disease | neurotoxicity | NMR | protein kinase | proteolysis

CDK5/p25 was first identified as a tau kinase (1, 2) that displayed a CDK1 (formerly $p34^{cdc2}$) -like substrate specificity in brain (3, 4). Of particular interest, phosphorylation of normal tau by CDK5/p25 could partially recapitulate several characteristics inherent to PHF-tau associated with Alzheimer's disease (1, 2). The CDK5 catalytic subunit was homologous to other CDKs and displayed ubiquitous expression (5), but p25 was originally discovered as a unique protein expressed predominantly in neurons, and generated by proteolytic cleavage of a larger protein precursor, p35 (6–9). Whereas CDK5/p35 is associated with normal neuron development and function (10), endogenous cleavage of p35 to p25 is associated with neuronal cell death, neuropathology, and is implicated in the progression of Alzheimer's disease (11–18), Parkinson's disease (19), and ALS (20). CDK5/p25, but not CDK5/p35, is toxic when overexpressed in transformed cell lines or when generated by cleavage of endogenous p35 in neurons (11, 21, 22). The cellular mechanism by which cleavage causes toxicity is not known, but in theory could relate to one or more known key differences between these two enzyme forms, including differences in subcellular distribution (11, 23), stability of the protein (11, 24), and/or cellular substrate specificity (11, 25).

There is common belief that the catalytic activity of CDK5/p25 is significantly elevated in comparison to CDK5/p35, and therefore that p25 causes "hyperactivity" of CDK5 compared to p35, contributing to its toxicity (10). To rigorously demonstrate its hyperactivity, however, it is necessary to show that the catalytic parameters associated with steady-state phosphorylation of substrates are different between the two enzymes. Hashiguchi et al. (26) previously conducted such experiments, and concluded that the intrinsic activity of CDK5/p25 was indeed significantly higher than that of CDK5/p35. Their data, however, consisted of few data points and was fraught with large errors.

We have reexamined the catalytic properties of CDK5 bound to p25 versus p35 by detailed kinetic analysis of the steady-state phosphorylation of histone H1 and human tau proteins. In contrast to the results of Hashiguchi et al. (26), we find that the kinetic parameters of both enzymes for the phosphorylation of these substrates are the same within experimental error. In addition, we have examined the phosphorylation of individual target sites in tau by two-dimensional NMR. Without exception, we find that the steady-state kinetic parameters of CDK5/p25 and CDK5/p35 toward individual sites are the same. We conclude that the cellular toxicity of CDK5/p25 in vivo cannot be ascribed to significant differences in the catalytic parameters between these enzymes when measured in vitro.

Results

Initial Velocity Studies. The substrate that displays the highest catalytic efficiency for phosphorylation by CDK5/p25 (or CDK5/p35) in vitro is histone H1 protein (27). This, in large part, is due to the target sequence in H1, KTPKKAKK, that conforms to the optimal consensus sequence motif for phosphorylation of substrates by this enzyme in general (27). To rigorously compare the catalytic efficiencies of CDK5/p25 vs. CDK5/p35, we sought to obtain values for $K_{m(H1)}$, $K_{m(\mathrm{ATP})}$, and k_{cat} for the phosphorylation of H1 histone for both enzymes. k_{cat} was determined from the $V_{\max}$ value corrected for the concentration of CDK5 catalytic subunit ($k_{\mathrm{cat}} = V_{\max}/[E]$) that was determined by slot blot analysis by using bacterially-expressed CDK5 of known concentration as a quantitative standard (*Materials and Methods*). The steady-state kinetic parameters for the phosphorylation of histone H1 were determined from initial velocity studies in which the concentrations of H1 and ATP were simultaneously varied.

CDK5/p25 could be easily expressed and purified from E. coli. However, expression of CDK5/p35 resulted in the p35 subunit consistently undergoing proteolytic degradation that in our hands could not be prevented. Thus, we could obtain kinetic information for E. coli-expressed CDK5/p25 only. The steady-state kinetic parameter values toward histone H1 were determined to be: $K_{m(H1)} = 30$ uM, $K_{m(\mathrm{ATP})} = 70$ uM, $k_{\mathrm{cat}} = 3\ \mathrm{sec}^{-1}$.

To compare CDK5/p25 to CDK5/p35, we employed baculovirus-expressed enzymes that were obtained from commercial source. Initial velocity data was collected on both enzymes and the model that best fit the data (Fig. S1) gave kinetic values

Author contributions: D.W.P., D.M.A., and D.A.T. performed research; D.W.P., H.Z., F.W.D., and J.L. analyzed data; H.Z. and F.W.D. contributed new reagents/analytic tools; J.L. designed research; and J.L. wrote the paper.

The authors declare no conflict of interest.

*This Direct Submission article had a prearranged editor

[1]To whom correspondence should be addressed. E-mail: lew@lifesci.ucsb.edu

This article contains supporting information online at www.pnas.org/cgi/content/full/0912718107/DCSupplemental.

www.pnas.org/cgi/doi/10.1073/pnas.0912718107

Table 1. Phosphorylation of kistone H1 by CDK5

	p25	p35
k_{cat} (s^{-1})	2.4 (1.4)†	2.1 (0.9)
$K_{m(H1)}$ (uM)	25 (4.4)	26 (4.7)
$K_{m(ATP)}$ (uM)	53 (10)	101 (17)

†Numbers in parenthesis are ± standard deviation

Table 2. Phosphorylation of tau by CDK5

	p25	p35
k_{cat} (s^{-1})	4.8 (2.4)†	4.6 (0.92)
$K_{m(tau)}$ (uM)	835 (454)	549 (118)
$k_{cat}/K_{m(tau)}$ (uM^{-1} min^{-1})‡	0.37 (0.02)	0.47 (0.02)
$K_{m(ATP)}$ (uM)‡	31 (9)	35 (6)

†Numbers in parenthesis are ± standard deviation.
‡Determined by measurement of initial slopes from Fig. 1*C* and *D* (*Materials & Methods*).

shown in Table 1. No significant differences in the k_{cat} value, nor in the K_m values for H1 or ATP, were found. Therefore, the overall catalytic efficiencies (k_{cat}/K_m) of both enzymes for histone phosphorylation appear to be similar. Furthermore, the kinetic constants of the baculovirus-expressed enzymes were similar to those of CDK5/p25 expressed in bacteria.

While H1 is catalytically the best substrate for several CDK/cyclin complexes in vitro, it is not known if its phosphorylation by CDK5 is physiologically relevant in neurons. Among substrates believed to be in vivo targets of CDK5, phosphorylation of the microtubule-associated protein, tau, has been of broad interest, because the sites on tau that are targeted by CDK5/p25 in vitro (1, 28–32) correspond to a subset of the specific sites in PHF-tau that are believed to be abnormally phosphorylated in AD brain (33–37). We, therefore, chose full-length human tau as a physiologically significant model substrate by which to compare the catalytic activities of CDK5/p25 and CDK5/p35.

Steady-state kinetic studies were conducted on both CDK5/p25 and CDK5/p35 as described for the phosphorylation of H1 but, instead, the longest isoform of human tau (441 amino acids) was used as substrate. We found that tau displayed extremely poor kinetics of phosphorylation catalyzed by either enzyme (Fig. 1). Upon fitting, the $K_{m(tau)}$ values were found to be in the 500–800 uM range, and saturating levels of tau could not be employed. Thus, the value for $K_{m(tau)}$ contained intrinsically large standard errors, and it was not possible to determine $K_{m(ATP)}$ by global fitting (Table 2). To more accurately determine catalytic efficiency ($k_{cat}/K_{m(tau)}$), we measured the initial slopes of the curves in Figure 1 and extrapolated to infinite ATP concentration. The resulting values suggest that the catalytic efficiency of CDK5/p25 was no greater than that of CDK5/p35; if anything it was lower (Table 2). The same analysis also revealed that the K_m values for ATP were the same (Table 2).

The observed poor kinetics of tau phosphorylation may be somewhat expected, given the consensus sequence motifs that surround each of the known CDK5/p25 phosphorylation sites in the tau molecule, all of which are theoretically poor sites for recognition (27). However, the poor catalytic efficiency in our hands concerned us, because other laboratories have reported significantly lower Km values for tau phosphorylation by CDK5/p25 (26, 38, 39). We reasoned that the poor catalytic efficiency could not be due to defects in the enzyme, because both CDK5/p25 and CDK5/p35 each displayed high activity toward histone H1. We investigated a number of parameters that may influence catalytic efficiency, including the concentrations of $MgCl_2$ and NaCl, the affect of heparin, the pretreatment of tau with heat, reduction by DTT, and the presence of the His_6 tag. We also tested if the state of tau aggregation was important by testing the efficiency of tau phosphorylation at various intermediate time points during the time course of tau aggregation into fibers. None of these parameters, nor different tau preparations carried out under non-denaturing versus denaturing conditions, appeared to affect the efficiency of tau phosphorylation by CDK5/p25 or CDK5/p35.

To conclusively demonstrate whether the poor kinetics was an artifact of tau expression, purification or handling or, in contrast, was a property intrinsic to tau itself, we engineered tau mutants in which the consensus sequences surrounding several established phosphorylation sites (40) were optimized for phosphorylation by CDK5. The corresponding wild-type and optimized consensus sequences are shown in Table 3. We reasoned that if the optimized mutant displayed dramatically enhanced catalytic efficiency, the poor efficiency of the wild-type substrate must necessarily be an intrinsic property of the primary structure alone. When we individually optimized the consensus sequences surrounding Ser235, Ser202 and Thr205, the K_m values decreased between 6-25 fold over wild-type tau whereas the catalytic efficiency (k_{cat}/K_m) was increased 5-11 fold. The fact that the wild-type and optimized mutants were overexpressed, purified,

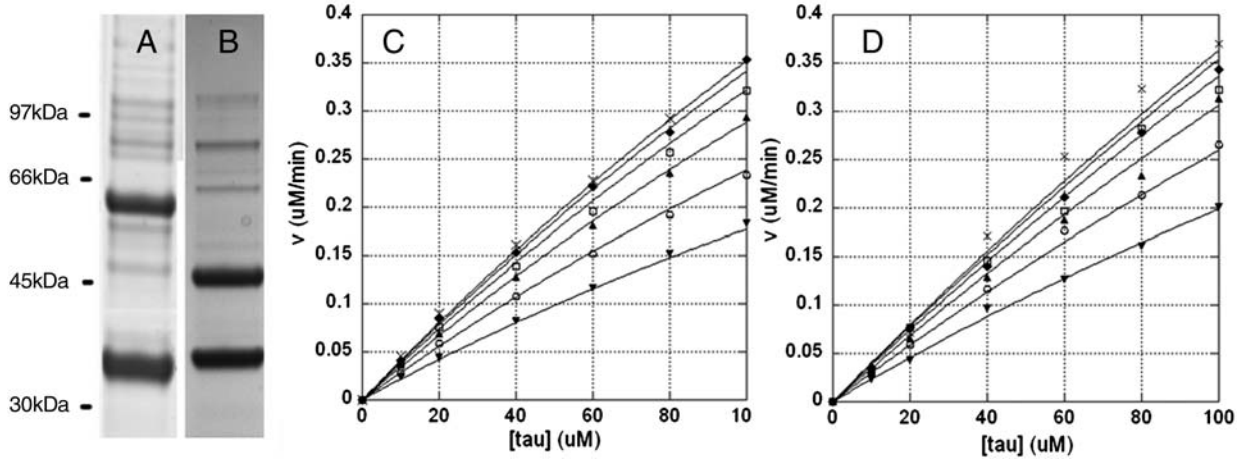

Fig. 1. Steady-state kinetic analysis of tau phosphorylation by CDK5 bound to p35 or p25. *A*, *B*) SDS-PAGE analysis of baculovirus expressed His_6CDK5/GSTp35 (*A*) and His_6CDK5/GSTp25 (*B*). Enzymes were purchased from Millipore. (*C*, *D*) Kinetic analysis of tau phosphorylation by His_6CDK5/GSTp35 (8.5 nM) (*C*) and His_6CDK5/GSTp25 (12 nM) (*D*). Initial rates were obtained in response to varying both tau and ATP concentrations. Data were analyzed by global nonlinear regression fitting to give the best-fit parameters in Table 2. In both *C* and *D*, ATP concentrations are (from top to bottom): *1 mM* -x, *500* -◆, *250* -□, *125* -▲, *62.5* -○, and *31 uM* -▼

Table 3. Kinetic parameters for catalytically optimized tau mutants

	k_{cat} (s^{-1})	K_m (uM)
Wild-type Tau	4.8†	835†
Optimized Tau		
PKS^{235}PKKAKS‡	2.1	33
PKS^{235}PSSAKS§		
PGS^{202}PKKPGS	5.8	143
PGS^{202}PGTPGS		
PGT^{205}PKKRSR	2.4	80
PGT^{205}PGSRSR		
DTS^{404}PKKLSN	ND¶	ND
DTS^{404}PRHLSN		
Histone H1‖		
PKT PKKAKK	2.4	30

†Kinetic parameters for wild-type tau are a composite of the kinetics for all four sites.

‡Individual optimized tau concensus sequences are in bold.

§corresponding wild-type sequences are shown below the optimized sequences.

¶Could not be determined.

‖The best substrate consensus sequence for CDK5/p25 is found in histone H1 (27).

and handled identically suggests that the dramatically different kinetics must be due solely to the difference in primary sequence.

Phosphorylation of Individual Sites. Site-specific phosphorylation of tau in vitro has previously been monitored by chemical sequence analysis (1, 30), phosphoepitope-specific tau antibodies (28, 29), and by mass spectrometry (31, 32). We monitored the phosphorylation of all sites in the entire tau molecule simultaneously in real time, by two-dimensional NMR. Tau phosphorylation by CDK5/p25 or CDK5/p35 resulted in four newly appearing, well-resolved resonance peaks in the ^{1}H-^{15}N-HSQC spectrum of ^{15}N-labeled tau over a 20 hr time course. These are labeled as peaks one, two, three, and four in Fig. 2*D* and *E*. In both cases, peaks one, two, and three displayed similar, if not identical, kinetics to one another whereas the time course of peak four was appreciably slower (Fig. 2*C* and *F*). To identify the residues that, upon phosphorylation, give rise to these peaks, we monitored the phosphorylation of several tau mutants that were catalytically optimized at individual sites. We found that each mutant produced a single, distinct, enhanced resonance peak corresponding to one of the four peaks in wild-type tau (Fig. 3). We interpreted this to mean that each resonance peak corresponded to the phosphorylation of a specific site, and that the appearance of each peak could serve as a site-specific reporter of phosphorylation. The chemical shift of a given peak may directly correspond to that of the actual phosphoamino acid or, alternatively, may be the result of a specific but indirect effect of phosphorylation. Peaks one, two, three, and four correlated with the phosphorylation of Ser^{235}, Ser^{404}, Thr^{205}, and Ser^{202}, resp. Each of the catalytically optimized sites was phosphorylated significantly faster than the corresponding wild-type site, demonstrating that the optimized mutants were indeed catalytically more proficient (Fig. 3*G* and *H*). Critically, the phosphorylation kinetics of any one of the four sites in wild-type tau appeared similar, if not identical, when catalyzed by CDK5/p25 versus CDK5/p35.

Cleavage of CDK5/p35 to CDK5/p25 By Calpain. To rigorously control for the relative active site concentrations of CDK5/p35 and CDK5/p25 when comparing their activities, we generated CDK5/p25 by direct cleavage of CDK5/p35 with calpain, and compared the tau kinase activity before and after digestion. We performed these assays at low tau concentration, under which conditions the initial velocity corresponds to the enzyme catalytic efficiency (k_{cat}/K_m) (41). Calpain digestion resulted in 80% cleavage of p35 at the highest calpain concentration used without detectable proteolysis of CDK5. We found that the catalytic efficiency of CDK5 was essentially unchanged in response to calpain digestion in which p35 was progressively converted to p25 (Fig. 4). This supports the results of our kinetic determinations on CDK5/p35 and CDK5/p25 when separately expressed and purified, and demonstrates that both display the same steady-state kinetic parameters toward human tau or histone H1, within experimental error.

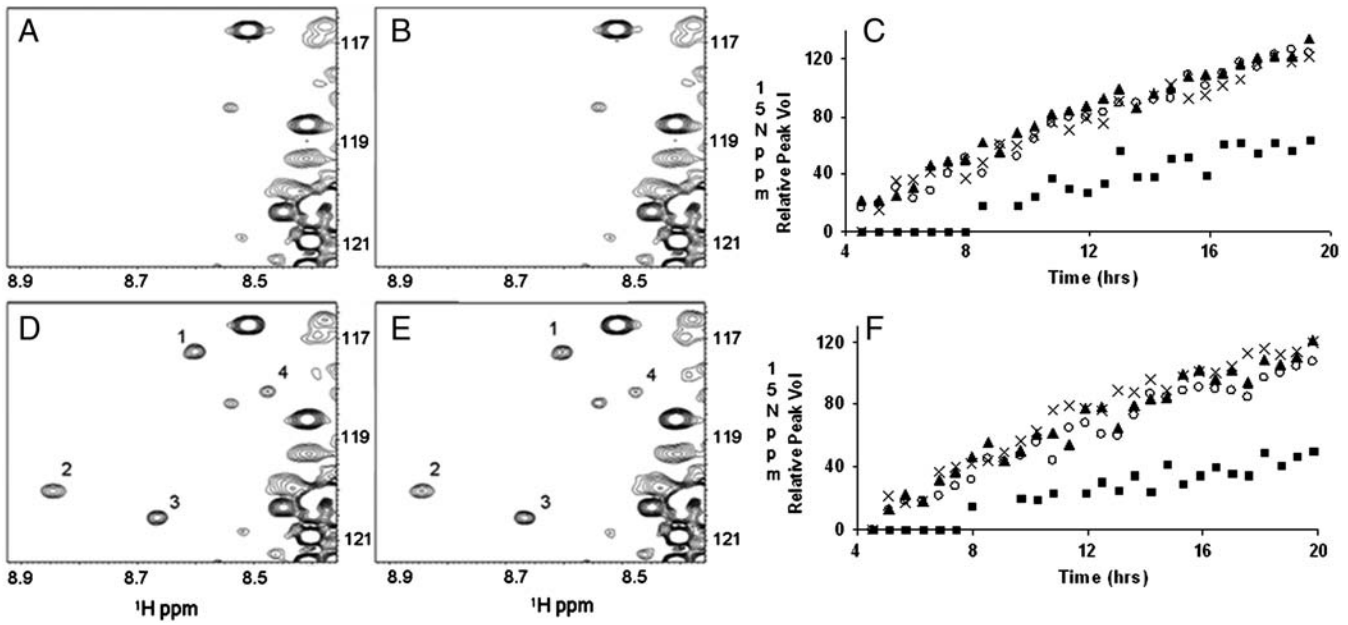

Fig. 2. ^{1}H-^{15}N-HSQC spectra of tau phosphorylated with CDK5/p35 or CDK5/p25. Region of new crosspeaks in response to phosphorylation by CDK5/p35 or CDK5/p25 is shown: *A*, *D*) CDK5/p35 (11 nM); *B*, *E*) CDK5/p25 (11 nM); *A*, *B*) after 30 min phosphorylation; *D*, *E*) after 19 hrs phosphorylation. New crosspeaks are labeled *1–4*; *C*, *F*) Time courses of phosphorylation monitored by increase in volume of crosspeaks *1–4*. *1* -○, *2* -▲, *3* -x, and *4* -■. *C*) CDK5/p35 *F*) CDK5/p25. The full NMR spectrum is shown in Fig. S2.

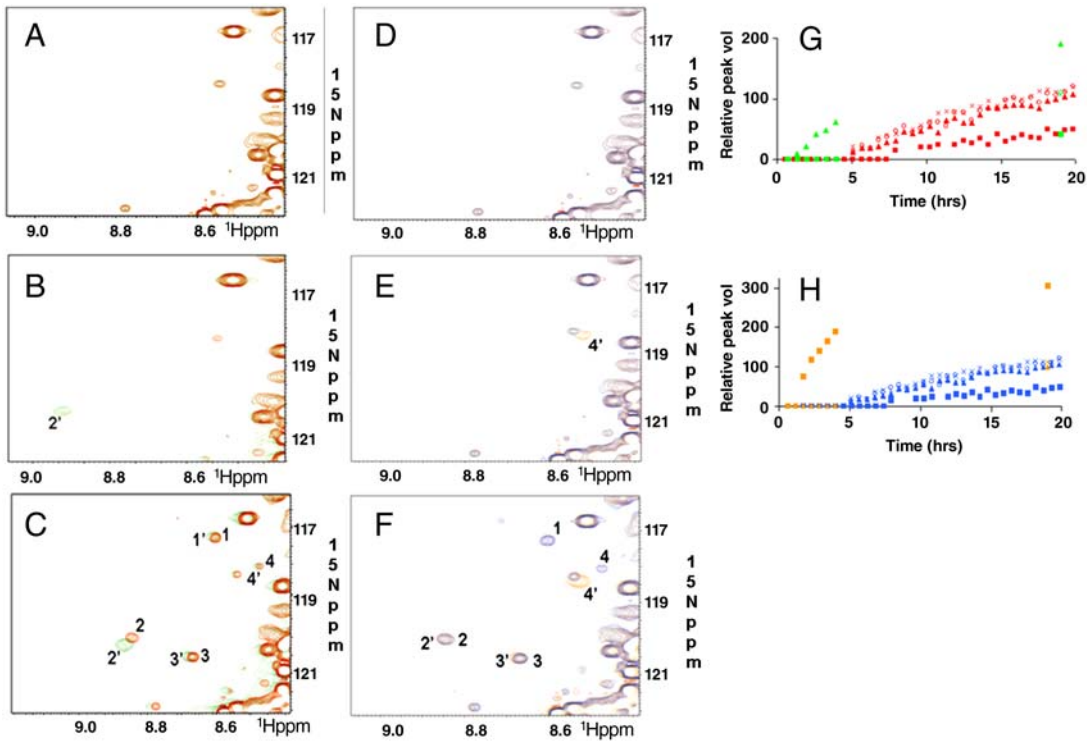

Fig. 3. CDK5/p25 phosphorylation-site optimization in tau. *A–C*) S^{235} The sequence S^{235}PSS was optimized for phosphorylation by CDK5/p25 by changing to S^{235}PKK. ^{1}H-^{15}N-HSQC spectra of S^{235}-optimized (*Green*) and wild type (*Red*) tau is shown after *A*) 0, *B*) 2, and *C*) 19 hrs phosphorylation by CDK5/p25 (11 nM). *G*) Relative change in peak volumes over time. *Red*—wild type; *Green*—mutant. *D–F*) S^{202} The sequence S^{202}PGT was optimized for phosphorylation by CDK5/p25 by changing to S^{202}PKK. ^{1}H-^{15}N-HSQC spectra of S^{202}-optimized (*Orange*) and wild-type (*Blue*) tau is shown after *D*) 0, *E*) 2, and *F*) 19 hrs phosphorylation by CDK5/p25 (11 nM). T^{205} is deleted; therefore peak 1′ is not seen. *H*) Relative change in peak volumes over time. *Blue*—wild-type; *Orange*—mutant. Peaks *1*, *2*, *3*, and *4*—wild-type tau. Peaks *1′*, *2′*, *3′*, and *4′*—catalytically optimized tau. *1,1′*,—pT^{205}; *2,2′*,—pS^{235}; *3,3′*,—pS^{404}; and *4,4′*,—pS^{202}.

Discussion

The link between p35 conversion to p25 and the incidence of Alzheimer's disease in humans remains controversial (11–17). However, many studies have now clearly implicated p25 in neurodegenerative disease in animal models (18–20, 42), and p25 causes neurotoxicity in cellular systems (11, 21, 22). The mechanism of toxicity specific to p25 versus p35 may be due to differences in a number of properties between CDK5/p25 and CDK5/p35 that have already been demonstrated, principally subcellular localization (11, 23) and stability (11, 24). In addition, there is common belief that CDK5/p25 is "hyperactive" compared to CDK5/p35, implying that the catalytic activity of CDK5 bound to p25 is enhanced compared to when bound to p35 (10, 11, 25, 26). This was previously demonstrated in cells in culture by using exogenously expressed tau as a substrate (11) and recently toward histone H1 (25). Subsequently, Hashiguchi et al employed steady-state kinetic methods to show that CDK5/p25 was catalytically more efficient than CDK5/p35 toward both histone H1 (3.5-fold) and human tau protein (6-fold) using purified components (26). These authors also examined the site-specific phosphorylation of tau by using phosphorylation site-specific antibodies, and found that phosphorylation of Ser^{202}/Thr^{205} was significantly preferred by CDK5/p25 compared to CDK5/p35 (26).

Herein, we have repeated the initial velocity studies of Hashiguchi et al. (26) and have employed NMR methods to monitor the simultaneous specific phosphorylation of individual sites in tau. In contrast to previous reports (26), we find that the catalytic parameters governing the steady-state phosphorylation of histone H1 and tau, and the phosphorylation of tau at specific sites, by CDK5/p25 or CDK5/p35, are virtually identical.

Hashiguchi et al. (26) reported steady-state kinetic parameter values that were associated with large errors in both cases of H1 and tau phosphorylation. We conducted the same experiments but collected more extensive data and found that neither the k_{cat} nor the K_m value for H1 or tau differed significantly between CDK5/p25 and CDK5/p35. Both enzymes were obtained from commercial sources by expression in baculovirus followed by purification by affinity-tag chromatography. In our hands, these enzymes displayed similar kinetic parameters to human CDK5/p25 expressed in E. coli, and the catalytic turnover rates were found to be similar to other CDKs using histone H1 as substrate (43). Both CDK5/p35 and CDK5/p25 displayed high, specific catalytic activity, as opposed to the possibility that they were compromised due to mishandling or trivial reasons.

We also monitored the phosphorylation of wild-type tau by NMR that allowed the kinetics of each site to be monitored in real time as they are simultaneously phosphorylated, as would be expected to occur in vivo. The disadvantage of this method, however, was that quantitative kinetic parameters could not be extracted because the relationship between resonance peak volume and phosphorylation stoichiometry could not be determined. Similar NMR experiments have recently been performed by Amniai et al. (44) using CDK2/cyclinA3 that shows similar substrate sequence specificity to CDK5/p25 (27, 45). They found Ser^{202}, Thr^{205}, Thr^{231}, and Ser^{235} as the major sites of tau phosphorylation by CDK2/cyclinA3 (44). We found tau to be phosphorylated primarily at Ser^{202}, Thr^{205}, Ser^{235}, and Ser^{404} by CDK5/p25. Whereas studies report as many as 25 sites capable of phosphorylation by CDK5/p25 (34), our NMR studies confirm the early work of Imahori et al. (40), who also demonstrated Ser^{202}, Thr^{205}, Ser^{235}, and Ser^{404} to be the major sites of tau phosphorylation by CDK5/p25 (tau kinase II). Critically, we found no difference in the kinetics of phosphorylation of each individual phosphorylation site—including Ser^{202}/Thr^{205}—by CDK5/p25 or CDK5/p35, in contrast to what Hashiguchi et al (26) have reported.

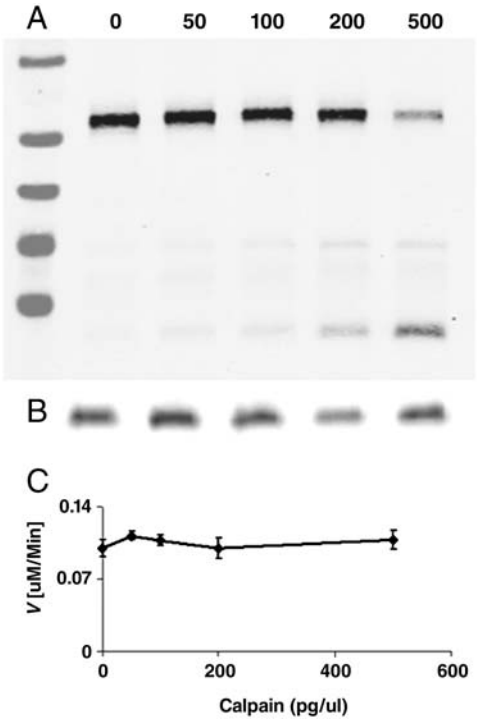

Fig. 4. Enzymatic activity of CDK5 upon conversion of p35 to p25 by calpain. Aliquots of CDK5/p35 were incubated with varying amounts of calpain, the reaction stopped with ALLN, and then assayed for tau kinase activity. *A*) Western blot of p35. Markers are 95, 72, 55, 43, and 34 kDa (top-bottom). *B*) Western blot of CDK5. *C*) Initial velocity of CDK5 (10 nM) after varied degrees of cleavage of p35 to p25. Cleavage of p35 to p25 results in no change in CDK5 catalytic efficiency.

In conclusion, we find that the catalytic efficiency and turnover rate of CDK5/p35 are not significantly changed towards either histone H1 or human tau protein upon cleavage to CDK5/p25 when measured using purified components. This is consistent with early work by Kusakawa et al,. who measured the activity of immunoprecipitates of these enzymes (46), and Sakaue et al., who tested both enzymes against several FTDP-17 mutants of tau (47). Recently, Maestras et al. (48) reported that CDK5/p25 is significantly more active than CDK5/p35 toward the anaphase-promoting complex factor, cdh1, suggesting that differential enzyme activity may be substrate-dependent. Alternatively, it is possible that intracellular protein–protein, protein–lipid interactions, or posttranslational modification may differentially affect catalytic specificity in vivo. For example, CDK5 has been reported to undergo phosphorylation at Tyr^{15} that increases activity (49). Otherwise, the toxicity of CDK5/p25 is likely attributed to its specifically altered subcellular compartmentalization and accessibility to different substrates. Our studies do not support hyperactivity of purified CDK5/p25 towards histone H1 or tau as a likely possibility.

Materials and Methods

Enzymes. Human CDK5/p25 and CDK5/p35 expressed in baculovirus were purchased from Millipore (Temecula, CA) or ProQinase (Freiburg, Germany). The purity of these enzymes is shown in Fig. 1. The concentration of CDK5 catalytic subunit was verified by quantitative Westernblot analysis. Briefly, a human CDK5 (N-terminal GST) standard was prepared by expression in E. coli, lysis by sonication (50% duty cycle, 60% power output), purification by centrifugation (15 k × 30 min), chromatography on GSH-agarose followed by Uno Q (0.5 ml/ min, 20 mM/ml NaCl gradient elution), and excision from a 10% SDS-PAGE gel and electro-elution from the gel chip by using an elu-Trap electro-elution apparatus. The GST-CDK5 protein was then precipitated with ethanol at −20° C and its concentration determined by UV absorbance ($\varepsilon_{280} = 75,010\ M^{-1}\ cm^{-1}$ based on amino acid composition). The GST-CDK5 was used as a quantitative standard to determine the picomole quantities of commercially obtained enzymes by slot blot analysis by using a CDK5-specific antibody (J3, Santa Cruz). Western blot analyses in Fig 4 were performed with anti-p25 (C19) and anti-CDK5 (J3) (Santa Cruz, CA). Calpain (C6108) was from Sigma. ALLN (BML-P120) was from Enzo Lifesciences, Plymouth Meeting, PA.

E. coli expression and purification of human CDK5/p25 was performed as follows: Human CDK5 and p25 were co-expressed in E. coli BL21(DE3) as GST- (pGEX2T) and His_6- (pET28) N-terminal fusion proteins under ampicillin and kanamycin resistance, resp. Cells were grown to OD_{600} 0.6 to 0.8 at 37 °C in LB, containing 50 ug/ml kanamycin and 100 ug/ml ampicillin, and then induced with 0.4 mM IPTG for 18 hrs at 22 °C. The cell pellet from 1 L culture was resuspended in 30 ml of lysis buffer (20 mM MOPS pH7.4, 500 mM NaCl and 0.1 mM EDTA, 1 mM DTT), washed with lysis buffer and then stored at −80° C until purification. Cells were thawed in lysis buffer, then incubated with lysozyme (2 mg/mL, 15 min on ice) in the presence of PMSF (1 mM), leupeptin (0.5 ug/ml) and pepstatin A (0.7 ug/ml), aprotinin 2 ug/ml), before sonication (Branson Sonifier 250, 6 × 20 sec at power setting five with 1 min cooling on ice between each sonication burst). The lysate after sonication was centrifuged (30 min at 15,000 rpm, Sorvall SS-34), supplemented with 0.5% Triton X100, then batch loaded onto 2 ml of packed GSH agarose at 4° C × 45 min. The resin was column washed with lysis buffer containing 0.5% Triton X100, followed by lysis buffer alone, and protein was eluted with 15 mM GSH.

The bound fraction was supplemented with 10 mM imidizole, batch loaded onto 2 mL packed Ni-NTA resin at 4 °C for 45 min, washed (20 mM MOPS pH7.4, 100 mM NaCl, 10 mM imidazole, 1 mM DTT and 0.1 mM EDTA), and bound protein eluted with 300 mM imidazole. The eluate was dialyzed against 20 mM MOPS pH7.4, 10 mM NaCl, 10 mM imidazole, 1 mM DTT and 0.1 mM EDTA, and then resolved by FPLC UnoQ anion exchange with a NaCl gradient (0–400 mM NaCl/20 mL). CDK5 kinase activity was assayed by using histone H1 protein as substrate. The corresponding GST-CDK5 protein was quantified by western analysis using a quantitative GST-CDK5 standard, as described above.

Protein Substrates. Histone H1 was from Sigma (H5505). Full-length ^{14}N and ^{15}N human tau (441 amino acids) containing a hexahistidine tag fused to the N terminus was overexpressed in E. coli and the protein purified according to Peterson et al. (50). Catalytically optimized mutants were generated by site directed mutagenesis by using QuickChange (Stratagene).

ATP. ATP (Sigma A2383) was dissolved in dilute NaOH such that the final pH of the stock ATP solution was between pH 6-7. The amount of ADP present was characterized by using a coupled, spectrophotometric assay (51), and was typically less than 1% of the total ATP. In all assays, radiolabeled [γ^{32}P-ATP] (MP Biomed 35001-X01) was used at final specific radioactivity of approximately 500 dpm/pmol. The exact specific radioactivity was determined by scintillation counting.

Initial Velocity Studies. Phosphorylation reactions were carried out at 37 °C in 20 mM MOPS pH 7.4, 50 mM KCl, 10 mM free MgCl, 1 mM DTT, varied γ^{32}P-ATP, and varied protein substrate concentrations. Enzyme concentration was in the 100 pM range, the precise concentration was adjusted to maintain initial velocity conditions (defined by conversion of 10% or less substrate to product). Reactions were terminated by addition of 25% (final concentration) acetic acid. γ^{32}P-ATP was separated from ^{32}P-labeled protein product by ascending chromatograpy on Whatman P81 phosphocellulose paper developed in 20 mM phosphoric acid (51). Radiolabeled product at the origin was quantified by Cerenkov counting.

Data Analysis. Initial velocity data (fixed and saturating ATP, varied H1, or tau) were fit to the Michaelis–Menten equation by simple nonlinear regression analysis by using Kaleidagraph (Synergy Software). Matrices of data (both ATP and H1 or tau varied) were analyzed by global nonlinear regression fitting by using a two substrate sequential model using the software program, Scientist (Micromath Scientific Software). V_{max} and K_m values were obtained directly from regression analysis. k_{cat} was calculated by dividing V_{max} by the CDK5 catalytic subunit concentration determined by Westernblot, as described above.

To determine catalytic efficiency ($k_{cat}/K_{m(tau)}$), each set of initial velocity data (Fig. 1), at a given subsaturating ATP concentration, was individually analyzed by hyperbolic nonlinear regression fitting. The initial slopes of each curve were replotted as a function of ATP concentration by using a hyperbolic model. The best-fit curve by nonlinear regression gave the catalytic efficiency ($k_{cat}/K_{m(tau)}$ at infinite ATP) and $K_{m(ATP)}$.

NMR. NMR data were collected at 25 °C on a Bruker Avance II 800 Ultrashield Plus NMR spectrometer by using either a 5 mm, four channel TCI

($^1H/^{15}N/^{13}C/^2H$) cryoprobe or a room temperature TXI H-C/N-D probe. We preformed two-dimensional ^1H-^{15}N HSQC experiments on uniformly ^{15}N-labeled protein samples of 250 uM full-length (441 amino acids) tau wild-type or mutants —purified as previously described [Peterson et al. (50)]— with 11nM CDK5-p35 or CDK5-p25 (ProQinase, Freiburg, Germany), in 20 mM MOPS pH 7.4, 100 mM NaCl, 0.1 mM EDTA, 2 mM DTT, 10 mM $MgCl_2$,10%/90% D_2O/H_2O, and 1 mM ATP. A ^1H-^{15}N HSQC spectrum was collected before ATP addition. After ATP addition, a series of ^1H-^{15}N HSQC spectra were collected continuously up to 20 h. Each spectrum was acquired over 34 mins and was done with eight scans, 100 ^{15}N increments, a recycle delay of 1 sec, and spectral width of 18.5 ppm for ^{15}N and 16.0 ppm for ^1H. There was a 5 min dead time between addition of ATP and data collection. Data processing was done with the nmrPipe program package (52). Data analysis was done with a modified version of Assignment of NMR Spectra by Interactive Graphics (53, 54) running under the Linux operating system.

ACKNOWLEDGMENTS. This work was supported by the National Institutes of Health Grant GM058445.

1. Ishiguro K, et al. (1991) A serine/threonine proline kinase activity is included in the tau protein kinase fraction forming a paired helical filament epitope. *Neurosci Lett* 128:195–8.
2. Ishiguro K, et al. (1992) Tau protein kinase I converts normal tau protein into A68-like component of paired helical filaments. *J Biol Chem* 267:10897–901.
3. Lew J, Beaudette K, Litwin CM, Wang JH (1992) Purification and characterization of a novel proline-directed protein kinase from bovine brain. *J Biol Chem* 267:13383–90.
4. Lew J, Winkfein RJ, Paudel HK, Wang JH (1992) Brain proline-directed protein kinase is a neurofilament kinase which displays high sequence homology to p34cdc2. *J Biol Chem* 267:25922–6.
5. Lew J, Wang JH (1995) Neuronal cdc2-like kinase. *Trends Biochem Sci* 20:33–7.
6. Ishiguro K, et al. (1994) Identification of the 23 kDa subunit of tau protein kinase II as a putative activator of cdk5 in bovine brain. *FEBS Lett* 342:203–8.
7. Lew J, et al. (1994) A brain-specific activator of cyclin-dependent kinase. *Nature* 371:423–6.
8. Tsai LH, Delalle I, Caviness VS, Jr, Chae T, Harlow E (1994) p35 is a neural-specific regulatory subunit of cyclin-dependent kinase 5. *Nature* 371:419–23.
9. Uchida T, et al. (1994) Precursor of cdk5 activator, the 23 kDa subunit of tau protein kinase II: its sequence and developmental change in brain. *FEBS Lett* 355:35–40.
10. Cruz JC, Tsai LH (2004) A Jekyll and Hyde kinase: roles for Cdk5 in brain development and disease. *Curr Opin Neurobiol* 14:390–4.
11. Patrick GN, et al. (1999) Conversion of p35 to p25 deregulates Cdk5 activity and promotes neurodegeneration. *Nature* 402:615–22.
12. Taniguchi S, et al. (2001) Calpain-mediated degradation of p35 to p25 in postmortem human and rat brains. *FEBS Lett* 489:46–50.
13. Takashima A, et al. (2001) Involvement of cyclin dependent kinase5 activator p25 on tau phosphorylation in mouse brain. *Neurosci Lett* 306:37–40.
14. Nguyen KC, Rosales JL, Barboza M, Lee KY (2002) Controversies over p25 in Alzheimer's disease. *J Alzheimers Dis* 4:123–6.
15. Yoo BC, Lubec G (2001) p25 protein in neurodegeneration. *Nature* 411:763–4 discussion 764-5.
16. Tandon A, et al. (2003) Brain levels of CDK5 activator p25 are not increased in Alzheimer's or other neurodegenerative diseases with neurofibrillary tangles. *J Neurochem* 86:572–81.
17. Tseng HC, Zhou Y, Shen Y, Tsai LH (2002) A survey of Cdk5 activator p35 and p25 levels in Alzheimer's disease brains. *FEBS Lett* 523:58–62.
18. Otth C, et al. (2002) AbetaPP induces cdk5-dependent tau hyperphosphorylation in transgenic mice Tg2576. *J Alzheimers Dis* 4:417–30.
19. Smith PD, et al. (2003) Cyclin-dependent kinase 5 is a mediator of dopaminergic neuron loss in a mouse model of Parkinson's disease. *P Natl Acad Sci USA* 100:13650–5.
20. Nguyen MD, Lariviere RC, Julien JP (2001) Deregulation of Cdk5 in a mouse model of ALS: toxicity alleviated by perikaryal neurofilament inclusions. *Neuron* 30:135–47.
21. Ahuja HS, Zhu Y, Zakeri Z (1997) Association of cyclin-dependent kinase 5 and its activator p35 with apoptotic cell death. *Dev Genet* 21:258–67.
22. Zhang J, Krishnamurthy PK, Johnson GV (2002) Cdk5 phosphorylates p53 and regulates its activity. *J Neurochem* 81:307–13.
23. Lee MS, et al. (2000) Neurotoxicity induces cleavage of p35 to p25 by calpain. *Nature* 405:360–4.
24. Patrick GN, Zhou P, Kwon YT, Howley PM, Tsai LH (1998) p35: the neuronal-specific activator of cyclin-dependent kinase 5 (Cdk5) is degraded by the ubiquitin-proteasome pathway. *J Biol Chem* 273:24057–64.
25. Kerokoski P, Suuronen T, Salminen A, Soininen H, Pirttila T (2002) Cleavage of the cyclin-dependent kinase 5 activator p35 to p25 does not induce tau hyperphosphorylation. *Biochem Biophys Res Commun* 298:693–8.
26. Hashiguchi M, Saito T, Hisanaga S, Hashiguchi T (2002) Truncation of CDK5 activator p35 induces intensive phosphorylation of Ser202/Thr205 of human tau. *J Biol Chem* 277:44525–30.
27. Beaudette KN, Lew J, Wang JH (1993) Substrate specificity characterization of a cdc2-like protein kinase purified from bovine brain. *J Biol Chem* 268:20825–30.
28. Baumann K, Mandelkow EM, Biernat J, Piwnica-Worms H, Mandelkow E (1993) Abnormal Alzheimer-like phosphorylation of tau-protein by cyclin-dependent kinases cdk2 and cdk5. *FEBS Lett* 336:417–24.
29. Ishiguro K, et al. (1995) Analysis of phosphorylation of tau with antibodies specific for phosphorylation sites. *Neurosci Lett* 202:81–4.
30. Paudel HK, Lew J, Ali Z, Wang JH (1993) Brain proline-directed protein kinase phosphorylates tau on sites that are abnormally phosphorylated in tau associated with Alzheimer's paired helical filaments. *J Biol Chem* 268:23512–8.
31. Lund ET, McKenna R, Evans DB, Sharma SK, Mathews WR (2001) Characterization of the in vitro phosphorylation of human tau by tau protein kinase II (cdk5/p20) using mass spectrometry. *J Neurochem* 76:1221–32.
32. Illenberger S, et al. (1998) The endogenous and cell cycle-dependent phosphorylation of tau protein in living cells: implications for Alzheimer's disease. *Mol Biol Cell* 9:1495–512.
33. Hasegawa M, et al. (1992) Protein sequence and mass spectrometric analyses of tau in the Alzheimer's disease brain. *J Biol Chem* 267:17047–54.
34. Hanger DP, Betts JC, Loviny TL, Blackstock WP, Anderton BH (1998) New phosphorylation sites identified in hyperphosphorylated tau (paired helical filament-tau) from Alzheimer's disease brain using nanoelectrospray mass spectrometry. *J Neurochem* 71:2465–76.
35. Morishima-Kawashima M, et al. (1995) Proline-directed and non-proline-directed phosphorylation of PHF-tau. *J Biol Chem* 270:823–9.
36. Hanger DP, et al. (2007) Novel phosphorylation sites in tau from Alzheimer brain support a role for casein kinase 1 in disease pathogenesis. *J Biol Chem* 282:23645–54.
37. Watanabe A, et al. (1993) In vivo phosphorylation sites in fetal and adult rat tau. *J Biol Chem* 268:25712–7.
38. Liu M, et al. (2008) Kinetic studies of Cdk5/p25 kinase: phosphorylation of tau and complex inhibition by two prototype inhibitors. *Biochemistry* 47:8367–77.
39. Ahn JS, et al. (2005) Defining Cdk5 ligand chemical space with small molecule inhibitors of tau phosphorylation. *Chem Biol* 12:811–23.
40. Imahori K, et al. (1998) Possible role of tau protein kinases in pathogenesis of Alzheimer's disease. *Neurobiol Aging* 19:S93–8.
41. Cornish-Bowden A (1995) *Fundamentals of Enzyme Kinetics* (Portland Press LTD, London).
42. Ahlijanian MK, et al. (2000) Hyperphosphorylated tau and neurofilament and cytoskeletal disruptions in mice overexpressing human p25, an activator of cdk5. *Proc Natl Acad Sci USA* 97:2910–5.
43. Lew J (2003) MAP kinases and CDKs: kinetic basis for catalytic activation. *Biochemistry* 42:849–56.
44. Amniai L, et al. (2009) Alzheimer disease specific phosphoepitopes of Tau interfere with assembly of tubulin but not binding to microtubules. *Faseb J* 23:1146–52.
45. Stevenson-Lindert LM, Fowler P, Lew J (2003) Substrate specificity of CDK2-cyclin A. What is optimal?. *J Biol Chem* 278:50956–60.
46. Kusakawa G, et al. (2000) Calpain-dependent proteolytic cleavage of the p35 cyclin-dependent kinase 5 activator to p25. *J Biol Chem* 275:17166–72.
47. Sakaue F, et al. (2005) Phosphorylation of FTDP-17 mutant tau by cyclin-dependent kinase 5 complexed with p35, p25, or p39. *J Biol Chem* 280:31522–9.
48. Maestre C, Delgado-Esteban M, Gomez-Sanchez JC, Bolanos JP, Almeida A (2008) Cdk5 phosphorylates Cdh1 and modulates cyclin B1 stability in excitotoxicity. *Embo J* 27:2736–45.
49. Zukerberg LR, et al. (2000) Cables links Cdk5 and c-Abl and facilitates Cdk5 tyrosine phosphorylation, kinase upregulation, and neurite outgrowth. *Neuron* 26:633–46.
50. Peterson DW, Zhou H, Dahlquist FW, Lew J (2008) A soluble oligomer of tau associated with fiber formation analyzed by NMR. *Biochemistry* 47:7393–404.
51. Prowse CN, Hagopian JC, Cobb MH, Ahn NG, Lew J (2000) Catalytic reaction pathway for the mitogen-activated protein kinase ERK2. *Biochemistry* 39:6258–66.
52. Delaglio F, et al. (1995) nmrPipe—a Multidimensional Spectral Processing System Based On Unix Pipes. *J Biomol NMR* 6:277–293.
53. Kraulis PJ (1989) ANSIG: A Program for the Assignment of Protein 1H 2D NMR spectra by Interactive Graphics. *J Magn Reson* 24:627–633.
54. Kraulis PJ, Domaille PJ, Campbell-Burk SL, Van Aken T, Laue ED (1994) Solution structure and dynamics of ras p21.GDP determined by heteronuclear three- and four-dimensional NMR spectroscopy. *Biochemistry* 33:3515–31.